

A NOVEL ARCHITECTURE FOR PEER-TO-PEER INTERCONNECT IN MILLIMETER-WAVE RADIO-OVER-FIBER ACCESS NETWORKS

J. Liu^{1,2,3}, L. Zhang^{3,4}, S.-H. Fan³, C. Guo², S. He^{1,2,*}, and G.-K. Chang³

¹Centre for Optical and Electromagnetic Research, State Key Laboratory of Modern Optical Instrumentation, Zhejiang University (ZJU), Hangzhou 310058, China

²ZJU-SCNU Joint Research Center of Photonics, South China Normal University (SCNU), Guangzhou 510006, China

³School of Electrical and Computer Engineering, Georgia Institute of Technology, Atlanta, GA 30332, USA

⁴State Key Lab of Advanced Optical Communication Systems and Networks, Department of Electronic Engineering, Shanghai Jiao Tong University, Shanghai 200240, China

Abstract—A novel peer-to-peer (P2P) interconnection architecture in a 60-GHz millimeter-wave (mm-wave) radio-over-fiber (RoF) access network is proposed for the first time. In this scheme, the beating of the lightwaves for downlink and P2P transmissions at the photodiode (PD) can provide signal up-conversion for both signals. Phase noise and frequency instability between the two independent lightwaves can be eliminated by a self-heterodyned radio frequency (RF) receiver (envelope detector) located on the user terminal, which can also down-convert simultaneously the two mm-wave signals to their associated intermediate frequencies. No high-frequency clock sources or other high bandwidth devices are required for signal up/down-conversions. A proof-of-concept experimental demonstration has also been carried out. Error-free transmission of the 1-Gb/ signals is achieved over 50-km fiber (downlink) or 25-km fiber (P2P) plus 4-m air link.

Received 27 January 2012, Accepted 5 March 2012, Scheduled 10 March 2012

* Corresponding author: Sailing He (sailing@kth.se).

1. INTRODUCTION

Multi-gigabit wireless over optical fiber networks using the radio-over-Fiber (RoF) technique have emerged as a powerful solution for increasing system capacity and mobility, as well as reducing the cost of access networks [1–5]. Nowadays, peer-to-peer (P2P) communication between wireless users in RoF access networks is increasingly useful due to the growth of applications such as multimedia communications, and voice and video over IP [6]. In these scenarios, the traffic from the source is sent to its nearest base station (BS), then sent to the BS close to the destination through the sub-network and finally delivered to the destination user. Compared with the traditional P2P communication in the wireless network, such wireless-optical-wireless communication mode can sustain the interference in wireless sub-network and thus improve the network throughput [7]. However, current schemes realizing P2P connection in the RoF access networks, especially the millimeter-wave (mm-wave) RoF access network [8, 9], require high frequency clock sources, high bandwidth modulators or lasers at the BS to achieve signal up-conversion, which increase the architecture complexity and cost on the user side [10, 11].

Recently, a self-heterodyne transmission technique was proposed for an mm-wave system in [12, 13], requiring no high-bandwidth millimeter-wave oscillator for frequency conversion to minimize the used devices and reduce the cost of the system. In this paper, we propose a novel P2P interconnection architecture by using the self-heterodyne transmission technique for 60-GHz mm-wave RoF access networks. In our scheme, the beating of the lightwaves for downlink and P2P transmission at the photodiode (PD) can provide signal up-conversion for both kinds of signals. An envelope detector (square-law-type detection) on the user terminal is used to down-convert the mm-wave signals and eliminate the frequency instability and poor phase-noise characteristics of the two independent signals. No high frequency clock sources or other high bandwidth devices are required for signal up/down-conversion. We also experimentally demonstrate and analyze the proposed scheme. Error-free transmission of the 1-Gb/ signals is achieved over 50-km fiber (downlink) or 25-km fiber (P2P) and 4-m air link.

2. PROPOSED ARCHITECTURE AND OPERATING PRINCIPLE

Figure 1(a) depicts the schematic diagram of the proposed P2P interconnection architecture in a 60-GHz mm-wave RoF access

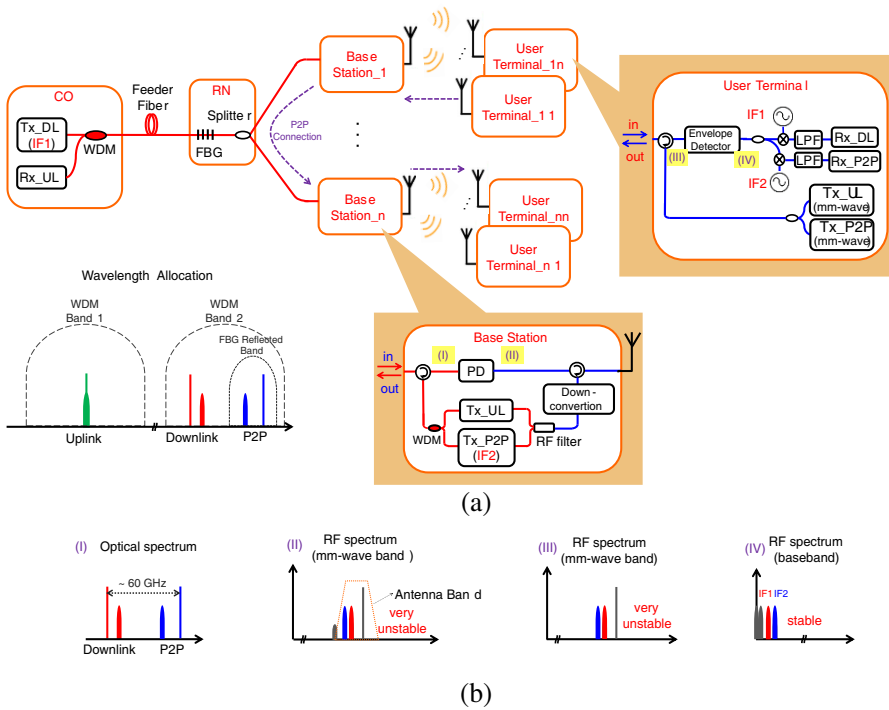


Figure 1. (a) Schematic diagram of the proposed P2P interconnection architecture in a 60-GHz mm-wave RoF access network; (b) Operating principle of downlink and P2P signal up/down-conversion. (CO: central office; Tx_DL: downlink transmitter; Rx_UL: uplink receiver; WDM: wavelength division multiplexer; Rx_DL: downlink receiver; Tx_UL: uplink transmitter; Tx_P2P: P2P transmitter; Rx_P2P: P2P receiver; LPF: low pass filter).

network. Here we assume one of the users (e.g., user terminal 11) attached to base station 1 (BS.1) would like to communicate with another user (e.g., user terminal nn) attached to base station BS.n. At the user terminal 11, the uplink and P2P signals at different mm-wave sub-bands are combined. After being transmitted through the antennas, the received signals are down-converted at BS.1. Here we note that the P2P signal is down-converted to an intermediate frequency (IF, e.g., IF2) rather than baseband. Then the obtained signals are modulated on two different wavelengths for the uplink and P2P transmission, respectively [see wavelength allocation in Fig. 1(a)]. At the remote node (RN), the P2P signal from user terminal 11 is

reflected using a fiber bragg grating (FBG) and broadcasted to all base stations through a 1: N power splitter. Then the downlink signal and P2P signal, between which the relative frequency spacing is around 60 GHz, beat at the PD of BS_n to up-convert both of the two signals to the 60-GHz mm-wave band for wireless transmission. After passing through the antennas, at the designated user terminal *mn* the received downlink and P2P signals are down-converted to their associated IFs by the envelope detector. This can help eliminate the frequency instability and poor phase-noise characteristics of the two independent optical signals. Then two RF clock sources, whose frequency are at IF1 and IF2, respectively, are used to separate the P2P signal from the downlink signal and thus realize the communication between the two wireless users. No high frequency clock sources or other high bandwidth devices are required for downlink and P2P signal up/down-conversion in our scheme.

Figure 1(b) illustrates the conceptual diagram of data up/down-conversion. The two coming optical signals before PD, as shown in inset (I), Fig. 1(b), can be approximated as:

$$E(t) = Ae^{j\omega_c t} + A_1(t) e^{j(\omega_c + \omega_{IF1})t} + B_1(t) e^{j[(\omega_c + \omega_f - \omega_{IF2})t + \theta(t)]} + Be^{j[(\omega_c + \omega_f)t + \theta(t)]} \quad (1)$$

Here A and B are amplitude of continuous wave (CW) lights from light sources used for downlink and P2P transmission, respectively; ω_c , ω_{IF1} and ω_{IF2} are the angular frequency of the CW light from downlink light source and intermediate RF frequency $IF1$ and $IF2$, respectively; ω_f , which is around 60 GHz, is the relative frequency between two CW lights, while $\theta(t)$ is the relative phase between the two free-running heterodyned light sources. $A_1(t)$ and $B_1(t)$ are downlink and P2P transmitting data, respectively. Single sideband signals are utilized here in order to decrease the useless sidebands generated through the beating of the two lights at PD as much as possible. After detected by the PD, the generated RF electrical signal at 60-GHz mm-wave band [see inset (II) of Fig. 1(b)] can be expressed as:

$$R(t) = 2\mu_1 AB \cos[\omega_f t + \theta(t)] + 2\mu_1 A_1(t) B \cos[(\omega_f - \omega_{IF1})t + \theta(t)] + 2\mu_1 AB_1(t) \cos[(\omega_f - \omega_{IF2})t + \theta(t)] + 2\mu_1 A_1(t) B_1(t) \cos[(\omega_f - \omega_{IF1} - \omega_{IF2})t + \theta(t)] \quad (2)$$

Here μ_1 is the response efficiency of the PD. $\theta(t)$, randomly changing with time and considered as phase noise, makes the generated mm-wave signals very unstable. After passing through the antennas, the undesired sideband [last term of (2)] is nearly filtered out [see inset

(III) of Fig. 1(b)]:

$$R_1(t) = 2\mu_1 AB \cos[\omega_f t + \theta(t)] + 2\mu_1 A_1(t) B \cos[(\omega_f - \omega_{IF1})t + \theta(t)] + 2\mu_1 AB_1(t) \cos[(\omega_f - \omega_{IF2})t + \theta(t)] \quad (3)$$

Then the envelope detector into which these signals are fed has its output at a low-frequency band [see inset (IV) of Fig. 1(b)]:

$$V(t) = \mu_2 |R_1(t)|^2 = 2\mu_1^2 \mu_2 A^2 B^2 + 2\mu_1^2 \mu_2 A_1^2(t) B^2 + 2\mu_1^2 \mu_2 A^2 B_1^2(t) + 4\mu_1^2 \mu_2 A B A_1(t) B_1(t) \cos(\omega_{IF1} - \omega_{IF2})t + 4\mu_1^2 \mu_2 A B^2 A_1(t) \cos\omega_{IF1}t + 4\mu_1^2 \mu_2 A^2 B B_1(t) \cos\omega_{IF2}t \quad (4)$$

μ_2 is the response efficiency of the envelope detector. The high frequency ($> IF2$) terms are eliminated due to the limited output bandwidth of the envelope detector. It can be found from the last two terms in (4) that the two desired signals at ω_{IF1} and ω_{IF2} do not include the phase-noise term $\theta(t)$ and is independent of the local-carrier frequency ω_f . Therefore, the frequency instability and poor phase-noise characteristics of the two free-running light sources will not have an impact on the final wanted signals.

3. EXPERIMENTAL SETUP

An experiment is carried out to verify the feasibility of the proposed scheme as illustrated in Fig. 2. Here we only perform the

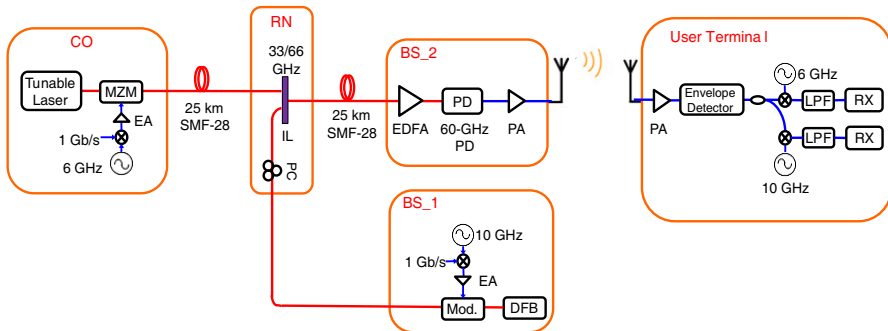


Figure 2. Experimental setup for realizing P2P interconnection in a 60-GHz mm-wave RoF access network. (MZM: Mach-Zehnder modulator; EA: electrical amplifier; PC: polarization controller; EDFA: erbium-doped fiber amplifier; PA: power amplifier; Mod.: modulator; DFB: distributed-feedback laser; RX: receiver).

demonstration for downlink and P2P transmission for simplification, since the uplink carrier is transmitted via a different WDM channel. For the downlink transmission, a 1-Gbit/s pseudo-random bit sequence (PRBS) stream, with a word length of $2^{23} - 1$ generated using a pulse pattern generator (PPG), is modulated on a CW light from a commercial tunable laser at an IF of 6 GHz. Then the generated IF signal is launched into a 25-km standard single-mode fiber (SSMF) to the RN. At the RN, the downlink signal is combined with the coming P2P light from BS_1 by a 33/66-GHz optical interleaver (IL) to realize single sideband transmission for the two signals. Then the combined signals are transmitted over a 25-km distribution SSMF into a 60-GHz PD at BS_2, generating mm-wave signals through the beating of the two carries. After transmitted over 4-m wireless distance, the received downlink and P2P signals at the user terminal are down-converted by an envelope detector (Millitech DXP-15) to their associated IF bands (the generated electrical spectrum is shown in Fig. 3(b)) and selected by the 6-GHz and 10-GHz local oscillators (LOs), respectively, for the BER evaluation.

4. RESULTS AND DISCUSSION

The optical spectra of the combined signals are shown in Fig. 3(a), from which we can see that the frequency spacing between the downlink and P2P carriers is around 65 GHz (0.52 nm). Considering the carrier-to-noise ratio [12] and carrier-to-intermodulation distortion [14] of system, the power ratio of the LO carrier to the RF signal was set to ~ 10 dB

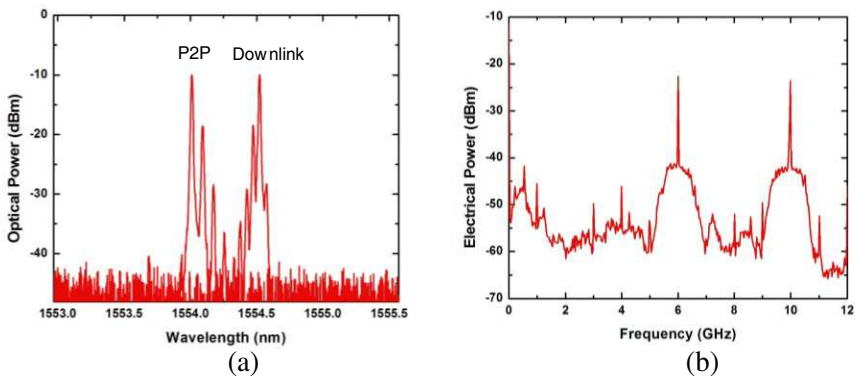


Figure 3. (a) Optical spectrum before PD; (b) Electrical spectrum after down-conversion by the envelope detector.

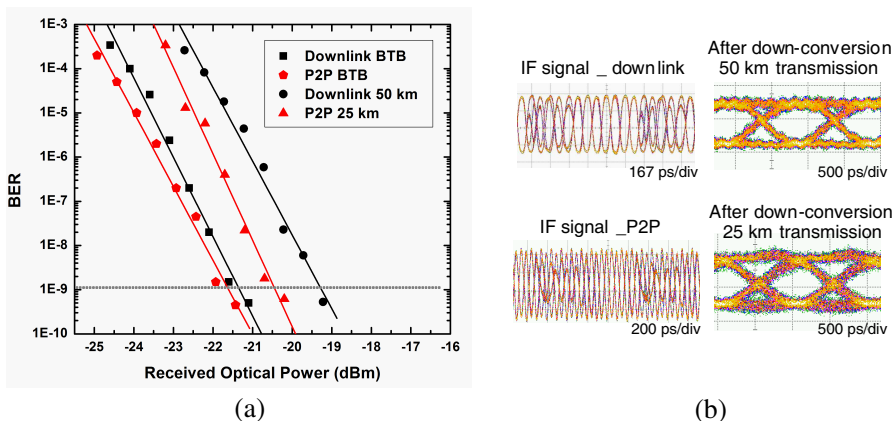


Figure 4. (a) BER curves and (b) eye diagrams for the downlink and P2P signals.

in our experiment. The electrical spectra of the signals after down-converting by the envelope detector are given in Fig. 3(b). Due to the bandwidth limitation of the spectrum analyzer, the ~ 60 -GHz RF spectra are not available here. Fig. 4(a) shows the bit-error-rate (BER) performance of the downlink and P2P signals, in both cases for back-to-back (BTB) and after 50-km (downlink) or 25-km (P2P) SSMF transmission. As shown in Fig. 4(a), compared with BTB case, the power penalty at BER of 10^{-9} is around 2 dB after transmission through the 50-km SSMF for the downlink transmission, while it is around 1 dB after 25-km SSMF transmission for the P2P transmission. The generated optical eye diagrams at the transmitters and the electrical eye diagrams after down-conversion at the receivers for both the downlink and P2P signals are provided in Fig. 4(b).

From (4) in Section 2, we can see the amplitude of the downlink signal at IF1 is proportional not only to the carrier amplitude of the downlink light source (A) but also to that of the P2P light source (B). Power ratio of the carrier to the RF signal of the downlink light source is often fixed in practical implementation. However, since the distances from RN to different base stations are not equivalent, different optical powers of the P2P signals from different base stations will be received at RN, which makes the received IF power of the downlink signal different. Here we assume that only one base station transmits the P2P signal at a certain time slot [15] and the optical transmitting powers of all the base stations are the same. Fig. 5 shows the measured relative received RF power at 6 GHz of the downlink signal versus different received optical power of the P2P signal before the PD. In the measurement,

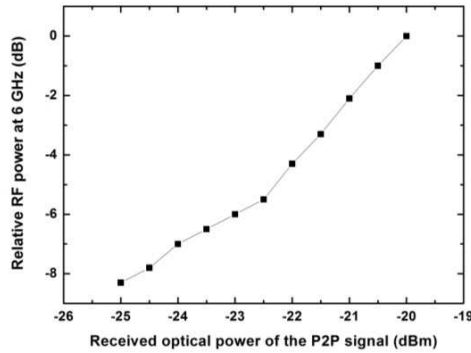


Figure 5. Relative received RF power at 6 GHz of downlink signal versus different received optical power of the P2P signal before the PD.

we keep the received optical power of the downlink signal before the PD constant, while adjusting the optical power of the P2P signal. Since the distribution-fiber-length difference is 25 km in the experiment and the typical power loss at 1550-nm band for the SMF is ~ 0.2 dB/km, the received power difference of the P2P signal is kept within 5 dB. When there is 5-dB optical power reduction of the received optical P2P signal, a ~ 8 -dB power loss is introduced to the received RF signal at 6 GHz for downlink transmission. Actually, in the practical implementation of the optical access network, the differential fiber length is often less than 10 km, so the received power difference of the P2P signal can be within 2 dB. According to the measured linear approximate curve in Fig. 5, an averagely ~ 3 -dB power loss is introduced to the received RF signal at 6 GHz for downlink transmission, when there is 2-dB optical power reduction of the received optical P2P signal. However, this power loss should be considered during system design.

Another issue should be considered in the proposed scheme is: if there is no P2P transmission during a certain period, how can we realize the downlink signal up-conversion? One of the solutions is that a specific light source for P2P transmission can also be turned on during some special time slots even when there is no P2P transmission. In this paper, we only realize a preliminary physical layer connection for P2P transmission. Issues such as P2P signal power adjustment for different base stations, signal security for the private connection between two users, transmission collision for different connecting path and Rayleigh back scattering for transmitting and receiving signals over the same fiber, can be supported by the higher layer protocols or algorithms, which will be the work of a future study.

5. CONCLUSION

We have proposed and experimentally demonstrated a novel P2P interconnection architecture in a 60-GHz mm-wave RoF access network for the first time. The beating of the lights for downlink and P2P transmission at the PD can realize signal up-conversion for both of these two signals. An envelope detector on the user terminal has been used to down-convert the mm-wave signals and eliminate the frequency instability and poor phase-noise characteristics of the two independent wavelengths. There is no complex architecture or high frequency clock source required to up/down-convert the downlink and P2P signals. Error-free transmission of the 1-Gb/s P2P (25-km fiber, 4-m wireless distance) and downlink (50-km fiber, 4-m wireless distance) signals has been realized in our experiment.

ACKNOWLEDGMENT

We are grateful to partial support of the Science and Technology Department of Zhejiang Province (2010R50007).

REFERENCES

1. Ogawa, H., D. Polifko, and S. Banba, "Millimeter wave fiber optics systems for personal radio communication," *IEEE Trans. Microw. Theory Tech.*, Vol. 40, No. 12, 2285–2293, 1992.
2. Jia, Z., J. Yu, G. Ellinas, and G.-K. Chang, "Key enabling technologies for optical-wireless networks: Optical millimeter-wave generation, wavelength reuse, and architecture," *J. Lightw. Technol.*, Vol. 25, No. 11, 3452–3471, 2007.
3. Nirmalathas, A., P. Gamage, C. Lim, D. Novak, and R. Waterhouse, "Digitized radio-over-fiber technologies for converged optical wireless access network," *J. Lightw. Technol.*, Vol. 28, No. 16, 2366–2375, 2010.
4. Fu, X., C. Cui, and S.-C. Chan, "Optically injected semiconductor laser for photonic microwave frequency mixing in radio-over-fiber," *Journal of Electromagnetic Waves and Applications*, Vol. 24, No. 7, 849–860, 2010.
5. Lu, H.-H., C.-Y. Li, C.-H. Lee, Y.-C. Hsiao, and H.-W. Chen, "Radio-over-fiber transport systems based on DFB LD with main and -1 side modes injection-locked technique," *Progress In Electromagnetics Research Letters*, Vol. 7, 25–33, 2009.

6. Narayanan, S. R., D. Braun, J. Buford, R. S. Fish, A. D. Gelman, A. Kaplan, R. Khandelwal, E. Shim, and H. Yu, "Peer-to-peer streaming for networked consumer electronics," *IEEE Communication Magazine*, Vol. 45, No. 6, 124–131, 2007.
7. Zheng, Z., J. Wang, and J. Wang, "A study of network throughput gain in optical-wireless (FiWi) networks subject to peer-to-peer communications," *IEEE International Conference on Communications*, 1–6, 2009.
8. Yang, B., X.-F. Jin, X.-M. Zhang, H. Chi, and S. L. Zheng, "Photonic generation of 60 GHz millimeter-wave by frequency quadrupling based on a mode-locking SOA fiber ring laser with a low modulation depth MZM," *Journal of Electromagnetic Waves and Applications*, Vol. 24, No. 13, 1773–1782, 2010.
9. Bakhtafrooz, A., A. Borji, D. Busuioc, and S. Safavi-Naeini, "Novel two-layer millimeter-wave slot array antennas based on substrate integrated waveguides," *Progress In Electromagnetics Research*, Vol. 109, 475–491, 2010.
10. Vegas Olmos, J. J., T. Kuri, T. Sono, K. Tamura, H. Toda, and K.-I. Kitayama, "Wireless and optical-integrated access network with peer-to-peer connection capability," *IEEE Photon. Technol. Lett.*, Vol. 20, No. 13, 1127–1129, 2008.
11. Li, Y., J. Wang, C. Qiao, A. Gumaste, Y. Xu, and Y. Xu, "Integrated fiber-wireless (FiWi) access networks supporting inter-ONU communications," *J. Lightw. Technol.*, Vol. 28, No. 5, 714–724, 2010.
12. Shoji, Y., K. Hamaguchi, and H. Ogawa, "Millimeter-wave remote self-heterodyne system for extremely stable and low-cost broadband signal transmission," *IEEE Trans. Microw. Theory Tech.*, Vol. 50, No. 6, 1458–1468, 2002.
13. Choi, C.-S., Y. Shoji, and H. Ogawa, "Millimeter-wave fiber-fed wireless access systems based on dense wavelength-division-multiplexing networks," *IEEE Trans. Microw. Theory Tech.*, Vol. 56, No. 1, 232–241, 2008.
14. Choi, C.-S. and Y. Shoji, "Third-order intermodulation distortion characteristics of millimeter-wave self-heterodyne transmission techniques," *Asia-Pacific Microw. Conf.*, 343–347, 2006.
15. Wong, E., and C.-J. Chae, "CSMA/CD-based ethernet passive optical network with optical internetworking capability among users," *IEEE Photon. Technol. Lett.*, Vol. 16, No. 9, 2195–2197, 2004.